Proceedings of Machine Learning Research vol vvv:1–15, 2024

System-level Safety Guard: Safe Tracking Control through Uncertain Neural Network Dynamics Models

Xiao Li HSIAOLI@UMICH.EDU
Yutong Li YUTLI@UMICH.EDU
Anouck Girard ANOUCK@UMICH.EDU
Ilya Kolmanovsky ILYA@UMICH.EDU
University of Michigan, Ann Arbor, MI, USA

Abstract

The Neural Network (NN), as a black-box function approximator, has been considered in many control and robotics applications. However, difficulties in verifying the overall system safety in the presence of uncertainties hinder the modular deployment of NN in safety-critical systems. In this paper, we leverage the NNs as predictive models for trajectory tracking of unknown dynamical systems. We consider controller design in the presence of both intrinsic uncertainty and uncertainties from other system modules. In this setting, we formulate the constrained trajectory tracking problem and show that it can be solved using Mixed-integer Linear Programming (MILP). The proposed MILP-based solution enjoys a provable safety guarantee for the overall system, and the approach is empirically demonstrated in robot navigation and obstacle avoidance through simulations. The demonstration videos are available at https://xiaolisean.github.io/publication/2023-11-01-L4DC2024.

Keywords: neural networks, system-level safety, uncertainties, trajectory tracking

1. Introduction

Robotic and autonomous driving systems are typically structured as a pipeline of individual modules, which are designed separately to satisfy corresponding performance requirements and are yet verified at a system level. With recent advances in machine learning, Neural Networks have been utilized to learn either individual modules, e.g., localization (Li et al. (2021)), mapping (Roddick and Cipolla (2020)), path planning (Barnes et al. (2017)), or learn the pipeline in an end-to-end fashion (Hu et al. (2023)). However, the NNs approximate the desired functionalities as nonlinear mappings from data introducing intrinsic approximation errors. On a system level, the performance of an NN module can also be affected by extrinsic uncertainties from other modules. In safety-critical robotics applications, the consideration of both intrinsic and extrinsic uncertainties is crucial to the module design, yet vital to securing safety at the system level.

Research has been dedicated to developing formal safety guarantees for robotic applications. The methods based on the Control Barrier Function (CBF) have been investigated to synthesize barrier functions to enforce safety constraints (Wang et al. (2018); Dai et al. (2017)). The CBFs have also been utilized to avoid collisions in robotic systems with NN-learned dynamics (Wei and Liu (2021)) and with an NN perception module (Tong et al. (2023)). However, the notion of uncertainties has not been considered in the literature above. In this work, we consider trajectory tracking controller design leveraging NNs as predictive models (see Figure 1). Apart from NN prediction errors, we consider the presence of uncertainties from other modules, which affect the NN predictions and, subsequently, impact the controller design and the system's safety.

Hewing et al. (2020) provides a review of techniques used to quantify and incorporate model uncertainties in control and robotic implementations. Probabilistic (Berkenkamp et al. (2016)) and

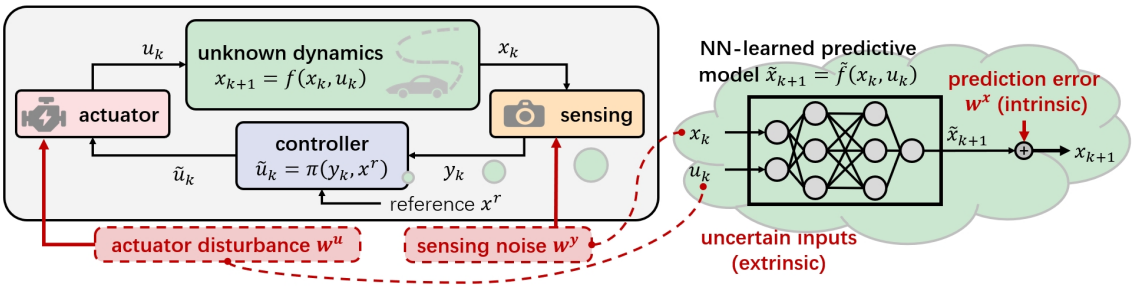

Figure 1: Trajectory tracking through an NN-learned predictive model: The controller leverages an NN-learned model (with prediction errors) for predicting the unknown dynamics and tracks the reference trajectories. The NN predictions depend on the states x_k before the sensing module and the control u_k out of the actuator module, which are not directly accessible by the controller in this pipeline, and are uncertain quantities due to sensing noises and actuator disturbances.

set-membership-based methods (Aswani et al. (2013)) have been considered to handle the uncertainties in nonlinear dynamic models. Methods have also been investigated to train NN modules with prediction confidence levels (Gal and Ghahramani (2016)). However, the literature has been focused on the module-level requirements. In this work, we design the tracking controller, accounting for system-level safety under both intrinsic and extrinsic uncertainties.

In a similar setting, robust controllers have been developed, that account for derived error bounds on perception modules (Dean et al. (2020, 2021); Dean and Recht (2021)). We assume that uncertainties are bounded within known sets. Differently from the existing literature, the uncertain inputs of the NN predictive model yield the activation status of NN neurons uncertain. We focus on exploiting the structure of NNs in accounting for uncertainty propagation. Semi-Definite Programming (SDP) (Hu et al. (2020)) has been used to assess the robustness of NN-based solutions. Unlike Hu et al. (2020), we consider the setting in which the NN inputs are affected by uncertainties that belong to a decision-variable-dependent set.

The contributions of this paper are as follows: 1) We propose an approach leveraging an NN-learned dynamic model for robust tracking controller design subject to system-level safety constraints. The safety and dynamics constraints are informed by uncertainty set propagation through NN and are handled using MILP. 2) We consider both intrinsic uncertainties from NN prediction errors and extrinsic uncertainties present in other modules and establish theoretical safety guarantees at the system level for the proposed method. 3) The theoretical properties are further demonstrated in simulations of collision-avoiding navigation of both omnidirectional robots and vehicles.

This paper is organized as follows: In Section 2, we introduce the assumptions on the actual dynamics of the system as well as the NN learned dynamics, and we formulate a robust tracking problem. In Section 3, we present our method to solve the robust tracking problem, using MILP and its theoretical properties. In Section 4, we use the proposed method, in combination with a Reachability-Guided RRT algorithm, to navigate a mass-point omnidirectional robot through a maze filled with obstacles. In Section 5, we leverage a set-theoretical localization algorithm that provides vehicle state measurements with uncertainty bounds, and we use our method to navigate a vehicle while avoiding collisions. Finally, conclusions are given in Section 6 and proofs of the theoretical properties are presented in Appendix A.

2. Problem Formulation

We consider a discrete-time dynamical system represented by $x_{k+1} = f(x_k, u_k)$, where $x_k \in \mathcal{X}$ is the state vector and $\mathcal{X} \subset \mathbb{R}^{n_x}$ is the state feasible set; $u_k \in \mathcal{U}$ is the control and $\mathcal{U} \subset \mathbb{R}^{n_u}$ is the control admissible set; and $f : \mathcal{X} \times \mathcal{U} \to \mathcal{X}$ is an unknown nonlinear mapping. In the sequel, we use lowercase letters, e.g., x, y, u, w, to represent vectors, capital letters, e.g., W, to define matrices, and scripted letters, e.g., $\mathcal{X}$,$\mathcal{U}$, to denote sets. We first discuss the neural network learned dynamic model for controller design that is subject to both intrinsic and extrinsic uncertainties in Section 2.1. Then, we introduce the robust tracking problem ensuring safety under uncertainties in Section 2.2.

2.1. Model Preliminaries

As shown in Figure 1, we approximate the dynamics f with a pre-trained $\ell-$layer fully connected neural network (NN) $\tilde{f} : \mathcal{X} \times \mathcal{U} \to \mathcal{X}$ that admits the following form

$$\begin{aligned} z_i = \sigma^{(i)}(\hat{z}_i), \quad \hat{z}_i = W^{(i)} z_{i-1} + b^{(i)}, \quad i = 1, \dots, \ell - 1, \\ z_0 = [x_k^T, u_k^T]^T, \quad \tilde{x}_{k+1} = W^{(\ell)} z_{\ell-1} + b^{(\ell)}, \end{aligned} \tag{1}$$

where $W^{(i)} \in \mathbb{R}^{n_i \times n_{i-1}}$, $b^{(i)} \in \mathbb{R}^{n_i}$ and $\sigma^{(i)} : \mathbb{R}^{n_i} \to \mathbb{R}^{n_i}$ are the weight matrix, the bias vector and an element-wise nonlinear activation function in the i^{th} layer, respectively. The NN uses the inputs x_k, u_k to compute a prediction $\tilde{x}_{k+1} = \tilde{f}(x_k, u_k)$ of the actual state x_{k+1}. We consider the overall system to be subject to uncertainties (see Figure 1) of three types: the NN prediction $\tilde{x}_{k+1}$ of the actual state x_{k+1} is subject to an unknown prediction error w_k^x, i.e.,

$$\tilde{x}_{k+1} = x_{k+1} + w_k^x, \ w_k^x \in \mathcal{W}_x, \tag{2}$$

where $\mathcal{W}_x \subset \mathbb{R}^{n_x}$ is a bounded set; moreover, the actual states x_k and the actual control input u_k are both latent to the controller due to the presence of noises in other modules. We assume that a state measurement y_k of the actual state x_k is available from the sensing module and admits the form

$$y_k = x_k + w_k^y, \ w_k^y \in \mathcal{W}_y, \tag{3}$$

where w_k^y is an unknown measurement noise, and $\mathcal{W}_y \subset \mathbb{R}^{n_x}$ is a bounded set. Meanwhile, we design a feedback controller $\pi : \mathcal{X} \times \mathcal{X} \to \mathcal{U}$ to track the reference state x^r. The actual control signal u_k is subject to an unknown additive actuator disturbance w_k^u, i.e.,

$$u_k = \tilde{u}_k + w_k^u, \ \tilde{u}_k = \pi(y_k, x^r), \ w_k^u \in \mathcal{W}_u, \tag{4}$$

where $\mathcal{W}_u \subset \mathbb{R}^{n_u}$ is a bounded set.

2.2. Robust Constrained Tracking Problem

Assume that there exists an unsafe subset $\mathcal{X}_u \subset \mathcal{X}$, e.g., representing obstacles, that the system should avoid. Given a reference $x^r \in \mathcal{X}_s$ in the safe complement subset $\mathcal{X}_s = \mathcal{X} \backslash \mathcal{X}_u$ and a state measurement y_k that obeys the assumption in (3), our task is to design a controller $\pi(y_k, x^r)$ to track the reference x^r while keeping the system in the safe subset $\mathcal{X}_s$, i.e., ensuring $x_{k+1} \in \mathcal{X}_s$ given $x_k \in \mathcal{X}_s$. These objectives can be accounted for by a constrained optimization problem,

$$\pi(y_k, x^r) = \underset{\tilde{u}_k}{\operatorname{argmin}} \left(\max_{x \in \mathcal{F}\left(\mathcal{X}_k, \mathcal{U}_k(\tilde{u}_k)\right)} \|x - x^r\|_p \right) \tag{5a}$$

$$\text{subject to:} \quad \tilde{u}_k \in \mathcal{U}, \ \mathcal{X}_k = (y_k \ominus \mathcal{W}_y) \cap \mathcal{X}_s, \ \mathcal{U}_k = \mathcal{U}_k(\tilde{u}_k) = (\tilde{u}_k \oplus \mathcal{W}_u) \cap \mathcal{U}, \tag{5b}$$

$$\tilde{\mathcal{F}}(\mathcal{X}_k, \mathcal{U}_k) = \left\{ \tilde{x}_{k+1} \in \mathcal{X} : \ \tilde{x}_{k+1} = \tilde{f}(x_k, u_k), \forall x_k \in \mathcal{X}_k, u_k \in \mathcal{U}_k \right\}, \tag{5c}$$

$$\mathcal{F}(\mathcal{X}_k,\mathcal{U}_k) = \tilde{\mathcal{F}}(\mathcal{X}_k,\mathcal{U}_k) \oplus \mathcal{W}_x,\ \mathcal{F}(\mathcal{X}_k,\mathcal{U}_k) \subset \mathcal{X}_s, \tag{5d}$$

where $\tilde{u}$ is the decision variable, $\|\cdot\|_p$ represents the ℓ_p norm, $\ominus$ represents the Pontryagin difference, and $\oplus$ denotes the Minkowski sum. The term $y_k \ominus \mathcal{W}_y$ stands for $\{y_k\} \ominus \mathcal{W}_y$ where we omit the curly brackets for simplicity. Given the measurement y_k that satisfies (3), the set $\mathcal{X}_k$ in constraint (5b) represents an uncertainty set that contains the actual state x_k. Similarly, the set $\mathcal{U}_k$ in constraint (5b) depends on the decision variable $\tilde{u}_k$ and contains the actual control u_k based on (4). The set-valued function $\tilde{\mathcal{F}} : \mathcal{X} \times \mathcal{U} \to \mathcal{X}$ in (5c) calculates the one step ahead reachable set of the learned NN dynamic model. The reachable set $\mathcal{F}(\mathcal{X}_k,\mathcal{U}_k)$ in (5d) is derived from $\tilde{\mathcal{F}}(\mathcal{X}_k,\mathcal{U}_k)$ and contains the actual state x_{k+1} based on (2). Meanwhile, the constraints in (5d) also guarantee the safety of the next state x_{k+1} for all the possible uncertainties modeled by (2), (3), (4). The objective defined by (5a) minimizes the maximum distance between the states in the reachable set $\mathcal{F}(\mathcal{X}_k,\mathcal{U}_k)$ and the reference, thereby steering the system closer to x^r. Unlike Hu et al. (2020), the input set $\mathcal{U}_k = \mathcal{U}_k(\tilde{u}_k)$ is conditioned on the decision variable $\tilde{u}_k$.

Remark *We introduce our methodology in the simplest possible setting, i.e., horizon-one Model Predictive Control with no control cost (Wei and Liu (2021)). The methodology can be extended to consider multiple prediction horizons, by augmenting (5c) and (5d) with the following constraints:*

$$\mathcal{F}^{(i+1)} = \tilde{\mathcal{F}}^{(i+1)} \oplus \mathcal{W}_x,\ \mathcal{F}^{(i+1)} \subset \mathcal{X}_s,\ \tilde{\mathcal{F}}^{(i+1)} = \tilde{\mathcal{F}}(\mathcal{F}^{(i)},\mathcal{U}_k),\ i = 1, 2, \ldots, N-1,$$

where N is the number of prediction horizons, and $\mathcal{F}^{(1)} = \mathcal{F}(\mathcal{X}_k,\mathcal{U}_k)$. We consider $p = 1$ in the sequel due to its convenient transcription to linear constraints. We also note that the objective function can use arbitrary ℓ_p norm and consider additive control cost.

3. Mixed-integer Linear Programming

To simplify the exposition of the approach, we assume the uncertainty sets in (2), (3), (4) are hyper-cubes defined according to

$$\mathcal{W}_x = \{w^x \in \mathbb{R}^{n_x} : |w^x| \le \epsilon^x,\ \epsilon^x \in \mathbb{R}^{n_x},\ \epsilon^x \ge 0\}, \tag{6a}$$

$$\mathcal{W}_y = \{w^y \in \mathbb{R}^{n_x} : |w^y| \le \epsilon^y,\ \epsilon^y \in \mathbb{R}^{n_x},\ \epsilon^y \ge 0\}, \tag{6b}$$

$$\mathcal{W}_u = \{w^u \in \mathbb{R}^{n_u} : |w^u| \le \epsilon^u,\ \epsilon^u \in \mathbb{R}^{n_u},\ \epsilon^u \ge 0\}. \tag{6c}$$

Note that, in principle, one can always find a hypercube overbounding a bounded set. Moreover, we assume the nonlinear functions in the NN model are ReLU activation functions

$$\sigma^{(i)}(x) = \texttt{ReLU}(x) = \max\{0, x\},\ i = 1, \cdots, \ell, \tag{7}$$

that are commonly adopted in different NN architectures and have good empirical performance (LeCun et al. (2015)). With a small abuse of notation, we use $a \le b$ to denote the element-wise order between two vectors $a, b \in \mathbb{R}^n$. In the sequel, given a lower bound $a \in \mathbb{R}^n$, an upper bound $b \in \mathbb{R}^n$ and $a \le b$, we use $[a, b]$ to denote a hypercube in $\mathbb{R}^n$. We use $I_{n\times n}$ to represent the identity matrix of size n. We use $\mathbb{1}_{n\times m}$, and $\mathbb{0}_{n\times m}$ to denote a matrix with all zeros and ones, respectively, of size $n \times m$. We neglect the subscript $n \times m$ in calculations assuming that the dimensions are appropriate. Meanwhile, we consider the state feasible set, control admissible set, and unsafe set according to

$$\mathcal{X} = [\underline{x}, \overline{x}],\ \underline{x}, \overline{x} \in \mathbb{R}^{n_x},\ \underline{x} \le \overline{x}, \tag{8a}$$

$$\mathcal{U} = [\underline{u}, \overline{u}],\ \underline{u}, \overline{u} \in \mathbb{R}^{n_u},\ \underline{u} \le \overline{u}, \tag{8b}$$

$$\mathcal{X}_u = \cup_i \mathcal{X}_u^{(i)},\ \mathcal{X}_u^{(i)} = [\underline{x}_u^{(i)}, \overline{x}_u^{(i)}],\ \underline{x}_u^{(i)}, \overline{x}_u^{(i)} \in \mathbb{R}^{n_x},\ \underline{x} \le \underline{x}_u^{(i)} \le \overline{x}_u^{(i)} \le \overline{x}. \tag{8c}$$

The definition of the unsafe set (8c) enables us to tightly over-bound obstacles of irregular shapes using unions of hypercubes in the optimization problem. Then, the equations (5b), (5c), (5d) encode the constraints associated with the input feasibility, NN structural non-linearity, and system safety, respectively, and are realized using integer decision variables as described in the respective Sections 3.1, 3.2, and 3.3. We also focus on the case when $p = 1$ in (5a), i.e., the cost function is based on the ℓ_1 norm, which leads to a MILP in Section 3.4. We prove that the formulated optimization constraints in this section can guarantee safety in Appendix A.

3.1. Constraints Embedding Input Feasibility

Given a measurement y_k and the decision variable $\tilde{u}_k$, the constraints (5b) define the sets $\mathcal{X}_k$, $\mathcal{U}_k$ that guarantee to contain the actual state x_k and the control u_k while the decision variable shall be admissible, i.e., $x_k \in \mathcal{X}_k$, $u_k \in \mathcal{U}_k$, $\tilde{u}_k \in \mathcal{U}_k$. We embed these feasibility conditions of the NN inputs using linear inequality and equality constraints in the following proposition.

Proposition 1 *Given state measurement y_k and a decision variable $\tilde{u}_k$, assume that the unknown actual quantities x_k and u_k obey (3), (4) with assumptions in (6b), (6c), (8a), (8b). Let the decision variables $\tilde{u}_k \in \mathbb{R}^{n_u}$, $a_0, b_0 \in \mathbb{R}^{n_x+n_u}$, and $\delta^a, \delta^b \in \mathbb{R}^{n_u}$ satisfy the following constraints*

$$a_{0,1:n_x} = \max\{\underline{x}, y_k - \epsilon^y\}, \quad b_{0,1:n_x} = \min\{\overline{x}, y_k + \epsilon^y\}, \quad a_0 \le b_0, \tag{9}$$

$$\begin{gathered} \underline{u} \le \tilde{u}_k \le \overline{u}, \quad \delta^a_j, \delta^b_j \in \{0,1\},\ j = 1, \dots, n_u, \\ \begin{cases} a_{0,(n_x+1):(n_x+n_u)} \ge \underline{u} \\ a_{0,(n_x+1):(n_x+n_u)} \ge \tilde{u}_k - \epsilon^u \\ a_{0,(n_x+1):(n_x+n_u)} \le \underline{u} + M(\mathbb{1} - \delta^a) \\ a_{0,(n_x+1):(n_x+n_u)} \le \tilde{u}_k - \epsilon^u + M\delta^a \end{cases}, \begin{cases} b_{0,(n_x+1):(n_x+n_u)} \le \overline{u} \\ b_{0,(n_x+1):(n_x+n_u)} \le \tilde{u}_k + \epsilon^u \\ b_{0,(n_x+1):(n_x+n_u)} \ge \overline{u} - M(\mathbb{1} - \delta^b) \\ b_{0,(n_x+1):(n_x+n_u)} \ge \tilde{u}_k + \epsilon^u - M\delta^b \end{cases}, \end{gathered} \tag{10}$$

where δ^a_j denotes the jth element in column vector δ^a, $a_{0,m:n}$ represents the vector containing elements between row n and row m in a_0, the constant matrix $M = \mathrm{Diag}\left(\max\{\epsilon^u, \overline{u} - \underline{u} - \epsilon^u\}\right)$, and $\mathrm{Diag}(x) \in \mathbb{R}^{n \times n}$ yields a square matrix with elements of x on the diagonal and zero anywhere else. Then, it is guaranteed that $z_0 = [x_k^T\ u_k^T]^T \in [a_0,\ b_0]$.

The constraints in Proposition 1 enforce input feasibility, i.e., $\tilde{u}_k \in \mathcal{U}_k$, and provide bounds a_0, b_0 to the NN input subject to extrinsic uncertainties, i.e., $a_0 \le [x^T,\ u^T]^T \le b_0$ for all $x \in \mathcal{X}_k,\ u \in \mathcal{U}_k$. Specifically, based on assumption (6b) and (8a), the constraints (9) imply $\mathcal{X}_k \subseteq [a_{0,1:n_x}, b_{0,1:n_x}]$. Based on assumption (6c) and (8b), the constraints (10) are equivalent to the following inequalities

$$\max\{\underline{u}, \tilde{u}_k - \epsilon^u\} = a_{0,(n_x+1)\cdots(n_x+n_u)} \le b_{0,(n_x+1)\cdots(n_x+n_u)} = \min\{\overline{u}, \tilde{u}_k + \epsilon^u\},$$

thereby $\mathcal{U}_k \subseteq [a_{0,(n_x+1):(n_x+n_u)}, b_{0,(n_x+1):(n_x+n_u)}]$. We use integer variables δ^a, δ^b to move the decision variable $\tilde{u}_k$ out of the nonlinear min/max function: $\delta^a_j = 1$ implies the jth element of $\max\{\underline{u}, \tilde{u}_k - \epsilon^u\}$ attains the value of the jth element of $\underline{u}$, otherwise $\delta^a_j = 0$; $\delta^b_j = 1$ indicates the jth element of $\min\{\overline{u}, \tilde{u}_k + \epsilon^u\}$ attains the value of the jth element of $\overline{u}$, otherwise $\delta^b_j = 0$. The proof is presented in A.1.

3.2. Constraints Encoding NN Structural Non-Linearity

Using the bounded sets $\mathcal{X}$ in (8a) and $\mathcal{U}$ in (8b), we can numerically derive lower and upper bounds $\underline{\hat{z}}_i, \overline{\hat{z}}_i \in \mathbb{R}^{n_i}, i = 1, \dots, \ell$ on the neuron values $\hat{z}_i$ and the output $\tilde{x}_{k+1}$ using interval arithmetic, i.e., $\hat{z}_i \in [\underline{\hat{z}}_i, \overline{\hat{z}}_i]$ and $\tilde{x}_{k+1} \in [\underline{\hat{z}}_\ell, \overline{\hat{z}}_\ell]$. In the sequel, these derived bounds are used to tighten the constraints and limit the search region for the optimization solver. Given the decision variables a_0, b_0 in Proposition 1 as bounds on the NN input, we can explicitly encode the variable uncertainty set propagation through the NN defined in (5c) using the following results:

Proposition 2 *Given $z_0 = [x_k^T \ u_k^T]^T \in [a_0, \ b_0]$, consider a NN defined by (1) and (7), and let the decision variables $a_{i-1}, b_{i-1} \in \mathbb{R}^{n_{i-1}}$, $\hat{a}_i, \hat{b}_i \in \mathbb{R}^{n_i}$, $\delta_i^{--}, \delta_i^{-+}, \delta_i^{++} \in \{0,1\}^{n_i}$, $i = 1, \dots, \ell-1$, and $a_{k+1}, b_{k+1} \in \mathbb{R}^{n_x}$ satisfy the following constraints*

$$\begin{gathered}\hat{a}_{i,j} = w_j^{(i)} S_i\left((w_j^{(i)})^T\right)\begin{bmatrix} a_{i-1} \\ b_{i-1}\end{bmatrix} + b_j^{(i)}, \quad \hat{b}_{i,j} = w_j^{(i)} S_i\left((w_j^{(i)})^T\right)\begin{bmatrix} b_{i-1} \\ a_{i-1}\end{bmatrix} + b_j^{(i)}, \\ \underline{\hat{z}}_i \le \hat{a}_i \le \hat{b}_i \le \overline{\hat{z}}_i, \quad \forall j = 1, \cdots, n_i, \quad \forall i = 1, \dots, \ell-1,\end{gathered} \tag{11}$$

$$\begin{gathered}\begin{cases} a_i \ge \hat{a}_i \\ a_i \le \hat{a}_i - \mathrm{Diag}(\underline{\hat{z}}_i)(\delta_i^{--} + \delta_i^{-+}) \\ a_i \le \mathrm{Diag}(\overline{\hat{z}}_i)\delta_i^{++}\end{cases}, \quad \begin{cases} b_i \ge \hat{b}_i \\ b_i \le \hat{b}_i - \mathrm{Diag}(\underline{\hat{z}}_i)\delta_i^{--} \\ b_i \le \mathrm{Diag}(\overline{\hat{z}}_i)(\delta_i^{-+} + \delta_i^{++})\end{cases}, \\ 0 \le a_i \le b_i, \quad \delta_{i,j}^{--}, \delta_{i,j}^{-+}, \delta_{i,j}^{++} \in \{0,1\}, \quad \delta_{i,j}^{--} + \delta_{i,j}^{-+} + \delta_{i,j}^{++} = 1, \\ \forall j = 1, \cdots, n_i, \quad \forall i = 1, \dots, \ell-1,\end{gathered} \tag{12}$$

$$\begin{gathered}\underline{\hat{z}}_\ell \le a_{k+1} \le b_{k+1} \le \overline{\hat{z}}_\ell, \quad a_{k+1,j} = w_j^{(\ell)} S_\ell\left((w_j^{(\ell)})^T\right)\begin{bmatrix} a_{\ell-1} \\ b_{\ell-1}\end{bmatrix} + b_j^{(\ell)}, \\ b_{k+1,j} = w_j^{(\ell)} S_\ell\left((w_j^{(\ell)})^T\right)\begin{bmatrix} b_{\ell-1} \\ a_{\ell-1}\end{bmatrix} + b_j^{(\ell)}, \quad \forall j = 1, \cdots, n_i,\end{gathered} \tag{13}$$

where $\hat{a}_{i,j}$ is the j^{th} element of $\hat{a}_i$; $w_j^{(i)}$ is the j^{th} row of $W^{(i)}$; $b_j^{(i)}$ is the j^{th} element of $b^{(i)}$; $\delta_{i,j}^{--}$ denotes the jth element of δ_i^{--}; $a_{k+1,j}, b_{k+1,j}$ represent the j^{th} element of a_{k+1}, b_{k+1}, respectively; The functions $S_i : \mathbb{R}^{n_{i-1}} \to \mathbb{R}^{n_{i-1} \times 2n_{i-1}}$ and $s : \mathbb{R} \to \mathbb{R}^{2n_{i-1}}$ are defined according to

$$S_i\left(\begin{bmatrix}\vdots \\ w_q \\ \vdots\end{bmatrix}\right) = \begin{bmatrix}\vdots \\ (s(w_q))^T \\ \vdots\end{bmatrix}, \quad s(w_q) := \begin{cases} \begin{bmatrix} e_q \\ \mathbb{0}_{n_{i-1}\times 1} \end{bmatrix} & \text{if } w_q \ge 0 \\ \begin{bmatrix} \mathbb{0}_{n_{i-1}\times 1} \\ e_q \end{bmatrix} & \text{if } w_q < 0 \end{cases},$$

and $e_q \in \mathbb{R}^{n_{i-1}}$ ($q = 1, \dots, n_{i-1}$) has 1 in the q^{th} element and zero anywhere else. Then, the variable reachable set $\tilde{\mathcal{F}}(\mathcal{X}_k, \mathcal{U}_k)$ defined in (5c) is a subset of hypercube $[a_{k+1}, b_{k+1}]$, i.e., $\tilde{\mathcal{F}}(\mathcal{X}_k, \mathcal{U}_k) \subseteq [a_{k+1}, b_{k+1}]$.

From the $(i-1)$th to ith layer of the NN, the uncertainty set propagation is realized through variables a_{i-1}, b_{i-1} and $\hat{a}_i, \hat{b}_i$ that are the lower and upper bounds of z_{i-1} and $\hat{z}_i$, respectively (i.e., $z_{i-1} \in [a_{i-1}, b_{i-1}]$ and $\hat{z}_i \in [\hat{a}_i, \hat{b}_i]$). The constraints (11) and (13) encode the uncertainty propagation through the fully connected layers, $\hat{z}_i = W^{(i)} z_{i-1} + b^{(i)}$ and $\tilde{x}_{k+1} = W^{(\ell)} z_{\ell-1} + b^{(\ell)}$, respectively. The uncertainty set propagation through the nonlinear ReLU function is enforced in constraints (12). In constraints (11) and (13), the qth row of matrix $S_i((w_j^{(i)})^T)$ switches the upper and lower bounds of z_{i-1} if the qth element in $w_j^{(i)}$ is negative. Meanwhile, since the values z_{i-1}

in neurons fall into a bounded hypercube $[a_{i-1}, b_{i-1}]$, the activation status of each ReLU activation function is uncertain. Inspired by Tjeng et al. (2017), we introduce integer variables $\delta_i^{--}, \delta_i^{-+}, \delta_i^{++}$ in constraints (12) to encode the uncertainty in the ReLU activation status according to

$$\hat{a}_{i,j} \leq \hat{b}_{i,j} \leq 0 \text{ if } \delta_{i,j}^{--} = 1; \quad \hat{a}_{i,j} \leq 0 \leq \hat{b}_{i,j} \text{ if } \delta_{i,j}^{-+} = 1; \quad 0 \leq \hat{a}_{i,j} \leq \hat{b}_{i,j} \text{ if } \delta_{i,j}^{++} = 1.$$

Furthermore, as can be shown, the hypercube defined by lower bound a_{k+1} and upper bound b_{k+1} is an over-estimation of the actual reachable set $\tilde{\mathcal{F}}$, i.e., $\tilde{\mathcal{F}} \subseteq [a_{k+1}, b_{k+1}]$. The proof is presented in Appendix A.2.

3.3. Constraints Enforcing System Safety

Given a hypercube $[a_{k+1}, b_{k+1}]$ as an over-estimation of the reachable set $\tilde{\mathcal{F}}$ in Proposition 2, we enforce the safety constrains (5d) of the system such that $x_{k+1} \in \mathcal{F}(\mathcal{X}_k, \mathcal{U}_k) \subset \mathcal{X}_s$. We consider the presence of a simple unsafe subset $\mathcal{X}_u = [\underline{x}_u, \overline{x}_u]$ in the following result and discuss the extension to a union of $\mathcal{X}_u^{(i)}$ defined in (8c) at the end of this section.

Proposition 3 *Given $\tilde{\mathcal{F}}(\mathcal{X}_k, \mathcal{U}_k) \subseteq [a_{k+1}, b_{k+1}]$ and state space defined in (8a), assume that the NN predictions are subject to bounded additive errors defined in (2) and (6a), and the decision variables $\underline{x}_{k+1}, \overline{x}_{k+1} \in \mathbb{R}^{n_x}$, $\delta_1^u, \delta_2^u \in \mathbb{R}^{n_x}$ satisfy the following constraints:*

$$\underline{x} \leq \underline{x}_{k+1} \leq \overline{x}_{k+1} \leq \overline{x}, \quad \underline{x}_{k+1} = a_{k+1} - \epsilon^x, \quad \overline{x}_{k+1} = b_{k+1} + \epsilon^x, \tag{14}$$

$$\begin{cases} \overline{x}_{k+1} \leq \overline{x} + \text{Diag}\left(\underline{x}_u - \overline{x}\right) \delta_1^u \\ \overline{x}_{k+1} \geq \underline{x}_u - \text{Diag}\left(\underline{x}_u - \underline{x}\right) \delta_1^u \\ \underline{x}_{k+1} \geq \underline{x} + \text{Diag}\left(\overline{x}_u - \underline{x}\right) \delta_2^u \\ \underline{x}_{k+1} \leq \overline{x}_u - \text{Diag}\left(\overline{x}_u - \overline{x}\right) \delta_2^u \end{cases}, \quad \begin{array}{c} \delta_{1,j}^u, \delta_{2,j}^u \in \{0,1\}, \quad \forall j = 1, \ldots, n_x, \\ \delta_{1,j}^u + \delta_{2,j}^u \leq 1, \quad \forall j = 1, \ldots, n_x, \\ \sum_{j=1}^{n_x} \left(\delta_{1,j}^u + \delta_{2,j}^u\right) \geq 1, \end{array} \tag{15}$$

where $\delta_{1,j}^u$, $\delta_{2,j}^u$ are the jth element of δ_1^u, δ_2^u, respectively. Then, $x_{k+1} \in \mathcal{F}(\mathcal{X}_k, \mathcal{U}_k)$ where $\mathcal{F}(\mathcal{X}_k, \mathcal{U}_k)$ is the reachable set defined in (5d), and $\mathcal{F}(\mathcal{X}_k, \mathcal{U}_k) \subseteq [\underline{x}_{k+1}, \overline{x}_{k+1}] \subset \mathcal{X}_s$ with $\mathcal{X}_u = [\underline{x}_u, \overline{x}_u]$.

In Proposition 3, the constraints (14) are equivalent to $[\underline{x}_{k+1}, \overline{x}_{k+1}] = [a_{k+1}, b_{k+1}] \oplus \mathcal{W}_x$ and $[\underline{x}_{k+1}, \overline{x}_{k+1}] \subset \mathcal{X}$. Considering the result $\tilde{\mathcal{F}}(\mathcal{X}_k, \mathcal{U}_k) \subseteq [a_{k+1}, b_{k+1}]$ from Proposition 2, it is obvious that $\mathcal{F}(\mathcal{X}_k, \mathcal{U}_k) \subseteq [\underline{x}_{k+1}, \overline{x}_{k+1}]$ based on the definition of $\mathcal{F}(\mathcal{X}_k, \mathcal{U}_k)$ in (5d). Subsequently, the safety constraint of $\mathcal{F}(\mathcal{X}_k, \mathcal{U}_k) \subset \mathcal{X}_s$ can be enforced with $[\underline{x}_{k+1}, \overline{x}_{k+1}] \subset \mathcal{X}_s$, which is equivalent to $[\underline{x}_{k+1}, \overline{x}_{k+1}] \subset \mathcal{X}$ and $[\underline{x}_{k+1}, \overline{x}_{k+1}] \cap \mathcal{X}_u = \varnothing$. The constraints (15) enforce $[\underline{x}_{k+1}, \overline{x}_{k+1}] \cap \mathcal{X}_u = \varnothing$ using integer variables according to

$$\begin{cases} \underline{x}_{k+1,j} \leq \overline{x}_{k+1,j} \leq \underline{x}_{u,j} & \text{if } \delta_{1,j}^u = 1, \ \delta_{2,j}^u = 0 \\ \overline{x}_{k+1,j} \geq \underline{x}_{k+1,j} \geq \overline{x}_{u,j} & \text{if } \delta_{1,j}^u = 0, \ \delta_{2,j}^u = 1 \\ \underline{x}_{u,j} \leq \overline{x}_{k+1,j} \leq \overline{x}, \ \underline{x} \leq \underline{x}_{k+1,j} \leq \overline{x}_{u,j} & \text{if } \delta_{1,j}^u = 0, \ \delta_{2,j}^u = 0 \end{cases},$$

where $\overline{x}_{k+1,j}, \underline{x}_{k+1,j}, \overline{x}_{u,j}, \underline{x}_{u,j}$ are the j^{th} element of $\overline{x}_{k+1}, \underline{x}_{k+1}, \overline{x}_u, \underline{x}_u$, respectively. The integer constraints imply that there exists at least one dimension j where $[\underline{x}_{k+1,j}, \overline{x}_{k+1,j}] \cap [\underline{x}_{u,j}, \overline{x}_{u,j}] = \varnothing$. Subsequently, the hypercube $[\underline{x}_{k+1}, \overline{x}_{k+1}]$ has zero overlaps with the unsafe subset $[\underline{x}_u, \overline{x}_u]$. Notably, in the case of a complex unsafe region $\mathcal{X}_u$, we can derive a union of hypercubes $\cup_i \mathcal{X}_u^{(i)}$ as in (8c) that over-bounds $\mathcal{X}_u$. Thereafter, to ensure safety, we can formulate similar constraints (15) with each individual hypercube $\mathcal{X}_u^{(i)}$ in the union. The proof is available in Appendix A.3.

3.4. Safe Tracking Control using MILP

The optimization objective in (5a) is designed to minimize the maximum distance between the points in the reachable set and the reference state x^r. Focusing on the case when $p = 1$, i.e., the cost is defined using ℓ_1 norm, we can introduce a vector of slack variables $\lambda \in \mathbb{R}^{n_x}$, and reformulate (5a) as

$$\begin{aligned} &\text{argmin}_{\tilde{u}_k} \textstyle\sum_{q=1}^{n_x} \lambda_q, \\ \text{subject to:} \quad &\lambda \geq 0,\ -\lambda \leq \underline{x}_{k+1} - x^r \leq \lambda,\ -\lambda \leq \overline{x}_{k+1} - x^r \leq \lambda, \end{aligned} \tag{16}$$

where λ_q designates the qth element of vector λ. This objective function relies on the fact that the maximum distance, between a reference x^r and points in the hypercube $[\underline{x}_{k+1}, \overline{x}_{k+1}]$, is attained at the points located at the boundary of the hypercube. Then, the optimization problem (5) for tracking the reference state x^r safely can be rewritten into a MILP according to

Robust Constrained Tracking Control Problem:

$$\begin{aligned} &\underset{\substack{\tilde{u}_k,\, \delta^a,\, \delta^b,\, a_0,\, b_0,\, a_{k+1},\, b_{k+1},\, \underline{x}_{k+1},\, \overline{x}_{k+1},\, \delta_1^u,\, \delta_2^u,\, \lambda, \\ a_i,\, b_i,\, \hat{a}_i,\, \hat{b}_i,\, \delta_i^{--},\, \delta_i^{-+},\, \delta_i^{++},\, i=1,\ldots,\ell-1,}}{\text{argmin}} \quad \sum_{q=1}^{n_x} \lambda_q, \\ &\text{subject to: (9), (10), (11), (12), (13), (14), (15), (16).} \end{aligned} \tag{17}$$

We note that the number of decision variables in the MILP problem (17) scales linearly with the number of neurons in the NN. In the subsequent examples, we use the *YALMIP* toolbox (Lofberg (2004)) for MATLAB to solve the optimization (17). It also has the following property. The proof is presented in Appendix A.

Proposition 4 *Consider a NN-learned dynamical system defined by (1), (7) that takes control u_k and state x_k as inputs and yields $\tilde{x}_{k+1}$ as a prediction of the next state x_{k+1} and satisfies the bounded additive error assumption in (2), (6a). We assume that $x_k \in \mathcal{X}_s$ is unknown but belongs to a safe set $\mathcal{X}_s = \mathcal{X} \backslash \mathcal{X}_u$ that is the complement set of the unsafe region $\mathcal{X}_u$ given by (8c) in the state space $\mathcal{X}$ defined by (8a). Also assume that a measurement y_k of x_k is given that satisfies the assumptions in (3), (6b). If there exists a solution of the Problem (17) such that the corresponding $\tilde{u}_k$ is in the admissible set $\mathcal{U}$ defined by (8b), then for all actuator disturbances w_k^u in set $\mathcal{W}_u$ defined by (6c), the actual control u_k subject to this additive disturbance w_k^u according to (4) renders the actual next system state safe, i.e., $x_{k+1} \in \mathcal{X}_s$.*

4. Obstacle Avoidance and Reachability-Guided RRT

We consider an omnidirectional robot as a mass point and use the following equation to represent its kinematics: $x_{k+1} = f(x_k, u_k) = x_k + u_k + w_k$, where $x_k \in \mathbb{R}^2$ is the robot coordinates in the $X - Y$ plane and $u_k \in \mathbb{R}^2$ contains the displacements, and the values of the disturbance $w_k \sim U(-\epsilon^x, \epsilon^x)$ are sampled uniformly from the interval $[-\epsilon^x, \epsilon^x]$. We use the sets $\mathcal{U} = \left\{[u_1\ u_2]^T \in \mathbb{R}^2 : -0.25 \leq u_1, u_2 \leq -0.25\right\}$, $\mathcal{X} = \left\{[x_1\ x_2]^T \in \mathbb{R}^2 : -1 \leq x_1, x_2 \leq 10\right\}$ together with obstacles $\mathcal{X}_u^{(i)}$ visualized in orange boxes in Figure 2. The NN is manually constructed and admits the following form

$$\tilde{x}_{k+1} = \begin{bmatrix} -I_{2\times 2} & -I_{2\times 2} \end{bmatrix} \texttt{ReLU}\left(\begin{bmatrix} I_{2\times 2} & \mathbb{0}_{2\times 2} \\ \mathbb{0}_{2\times 2} & I_{2\times 2} \end{bmatrix} \begin{bmatrix} x_k \\ u_k \end{bmatrix} + \begin{bmatrix} -50 \cdot \mathbb{1}_{2\times 1} \\ -50 \cdot \mathbb{1}_{2\times 1} \end{bmatrix} \right) + 100 \cdot \mathbb{1}_{2\times 1},$$

which is equivalent to $\tilde{x}_{k+1} = \tilde{f}(x_k, u_k) = x_k + u_k$ given $x_k \in \mathcal{X}$ and $u_k \in \mathcal{U}$. Finally, the uncertainty bounds are set to $\epsilon^x = \epsilon^u = \epsilon^y = [0.05,\ 0.05]^T$. We develop a reachability-guided RRT

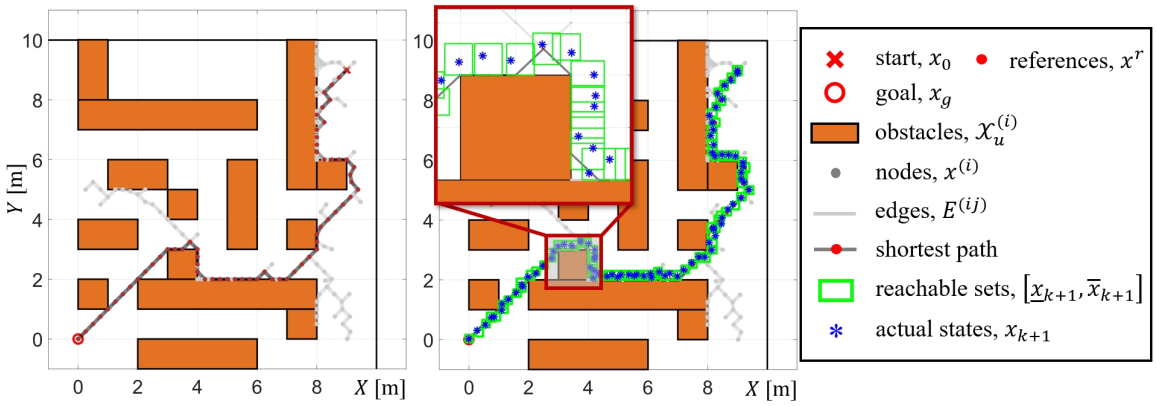

Figure 2: Schematic of obstacle avoidance using an omnidirectional robot: (Left) The reachability-guided RRT algorithm expands the tree from the start x_0 to the goal x_g over the safe state space $\mathcal{X}_s$. Then, we use the Dijkstra planning algorithm to find a reference path (black lines with red dots) from x_0 to x_g that has the shortest distance defined by ℓ_1 norm. (Middle) We use the proposed method in (17) to track the reference states (red dots). Our method can guarantee that the robot is collision-free under uncertainties, i.e., the unknown actual states in blue asterisks are in the safe set $\mathcal{X}_s$, even with most of the reference points located near the obstacles.

planner similar to Shkolnik et al. (2009), combined with the Dijkstra algorithm, to generate a path of reference states x^r. Different from the classic RRT, the reachability-guided RRT incorporates dynamics as a constraint to extend the edges of the tree. This tree $\mathcal{T}(\{x^{(i)}\}, \{E^{(ij)}\})$ comprises nodes $x^{(i)} \in \mathcal{X}_s$ and directed edges $E^{(ij)}$. The edge $E^{(ij)}$ connects node $x^{(i)}$ to node $x^{(j)}$ and implies that there exists a control $u_k \in \mathcal{U}$ such that $x^{(j)} = \tilde{f}(x^{(i)}, u_k) \in \mathcal{X}_s$, i.e., $x^{(j)} \in \tilde{\mathcal{F}}(\{x^{(i)}\}, \mathcal{U}) \cap \mathcal{X}_s$. As shown in Figure 2, the algorithm is initialized with an initial node x_0 and is terminated if there exists a node $x^{(i)} \in \mathcal{T}$ such that $x_g \in \tilde{\mathcal{F}}(\{x^{(i)}\}, \mathcal{U})$. At each time step, we take the first node $x^{(i)}$ in the shortest path as the reference state x^r in (17). We solve the optimization (17) and apply the resulting control $\tilde{u}_k$ to the actual dynamic model f. Then, we remove $x^{(i)}$ from the path if $x^{(i)} \in [\underline{x}_{k+1}, \overline{x}_{k+1}]$ and the navigation terminates when $x_g \in [\underline{x}_{k+1}, \overline{x}_{k+1}]$. As shown in Figure 2, after taking control $\tilde{u}_k$, the resulting next states x_{k+1} in blue asterisks are within the reachable set $[\underline{x}_{k+1}, \overline{x}_{k+1}]$ in green boxes and the boxes $[\underline{x}_{k+1}, \overline{x}_{k+1}]$ are collision-free, which empirically validates the Proposition 4.

5. Vehicle Navigation and Set-theoretical Localization

As shown in Figure 3, we consider a front-wheel drive vehicle of width 2 m. The length of the vehicle wheelbase is $l = 5$ m. We adopt the vehicle kinematics model from Li et al. (2023), which admits the form

$$x_{k+1} = f(x_k, u_k) = \begin{bmatrix} p_{x,k} + v_k dt \cos\theta_k \cos\delta_k \\ p_{x,k} + v_k dt \sin\theta_k \cos\delta_k \\ \theta_k + v_k dt/l \sin\delta_k \end{bmatrix},$$

where $x_k = [p_{x,k}\ p_{y,k}\ \theta_k]^T$ is the state vector, $(p_{x,k},\ p_{y,k})$ in meters are the coordinates of the center of the vehicle rear wheel axis, and $\theta_k \in [-\pi, \pi]$ is the vehicle orientation; $u_k = [v_k\ \delta_k]^T$ is the control vector, v_k in m/s is the vehicle longitudinal speed, and δ_k in rad is the vehicle steering angle; $dt = 0.1$ sec is the sampling period. We use the sets $\mathcal{U} = \{u_k : v_k \in [2, 5],\ \delta_k \in [-0.6, 0.6]\}$, $\mathcal{X} = \{x_k : p_{x,k}, p_{y,k} \in [-50, 50],\ \theta_k \in [-\pi, \pi]\}$ together with obstacles $\mathcal{X}_u^{(i)}$ visualized in grey boxes in Figure 3. For the uncertainties, we assume the actuator disturbance $\epsilon^u = [0.01\ \text{m/s},\ 0.5\ \text{deg}]^{\text{T}}$.

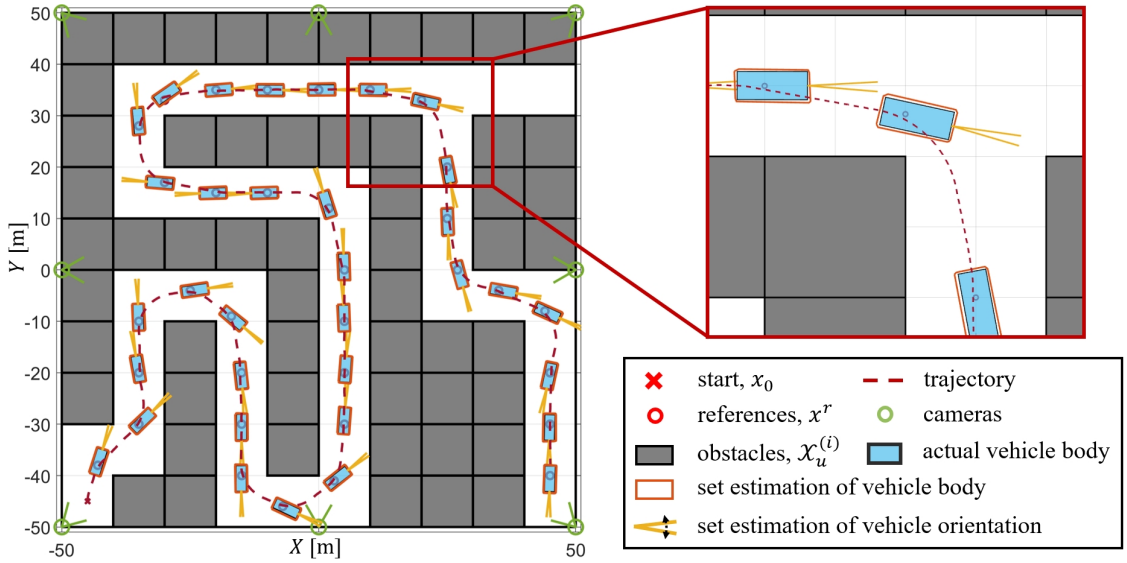

Figure 3: Schematic of navigating a vehicle through a maze with tracking controller (17) and with a set-theoretic localization algorithm. The zoom-in view, at the top-left, demonstrates that the set-theoretic localization algorithm provides estimates of the vehicle body and orientation that are guaranteed to contain the actual ones. The tracking controller (17) leverages this information, together with an NN-learned vehicle dynamics model, to avoid obstacles.

We densely sample a dataset $\mathcal{D} = \{(x_k^{(i)}, u_k^{(i)}, x_{k+1}^{(i)})\}_i$ from $\mathcal{X} \times \mathcal{U}$ for NN training and quantifying the NN prediction error. Based on Pytorch library(Paszke et al. (2019)), we train an NN $\tilde{f}$ using the Stochastic Gradient Descent algorithm and dataset $\mathcal{D}$ to minimize the mean-squared error $\left\| x_{k+1}^{(i)} - \tilde{f}(x_k^{(i)}, u_k^{(i)}) \right\|_2^2$, and the prediction error is equal to $\epsilon^x = [0.02 \text{ m}, \ 0.02 \text{ m}, \ 1.5 \text{ deg}]^{\mathrm{T}}$. We quantify the prediction error as the maximum value of the empirical absolute error, i.e.,

$$\epsilon^x = \max \left\{ \epsilon \in \mathbb{R}^3 : \epsilon = \left| x_{k+1}^{(i)} - \tilde{f}(x_k^{(i)}, u_k^{(i)}) \right|, \ (x_k^{(i)}, u_k^{(i)}, x_{k+1}^{(i)}) \in \mathcal{D} \right\},$$

and the function max is applied element-wise. The theoretical properties of uncertainty-bound quantification from samples are discussed in Dean et al. (2020) and are beyond the scope of this work. At each time step k, we apply the set-theoretic localization algorithm presented in Li et al. (2023) to generate an uncertainty polygon P_{xy} that contains the actual vehicle position $[p_{x,k}, \ p_{y,k}]^T$ and an uncertainty interval P_θ that contains the actual vehicle orientation θ_k, i.e., $[p_{x,k}, \ p_{y,k}]^T \in P_{xy}$ and $\theta_k \in P_\theta$. Subsequently, we can derive the smallest hypercube P that over-bounds $P_{xy} \times P_\theta$, and the measurement error ϵ^y is quantified as half of the sizes of P. The algorithm can also produce a polytope estimation of the vehicle body as demonstrated in Figure 3. Then, akin to the process in Section 4, we solve the optimization problem (17) and use the resulting control to navigate the vehicle through the maze. As shown in Figure 3, we can also observe that the vehicle is collision-free, which is guaranteed formally by Proposition 4.

6. Conclusion and Future Work

In this paper, we developed an approach for robust reference tracking that leveraged a learned NN model to control the actual dynamics. We considered both bounded intrinsic and extrinsic

uncertainties from the controller and other system modules, respectively. We transcripted the resulting variable uncertainty set propagation through NN using a MILP. We provided formal proof that the proposed MILP can render the overall system safe considering all possible actuator disturbances, measurement noise, and prediction errors within their corresponding bounded sets. We test the proposed method in navigation and obstacle avoidance of omnidirectional robots and vehicles in simulations. Future work will include the investigation of tightening the over-estimation by the hypercubes, and an extension to ensure the recursive feasibility and stability of the proposed MILP.

References

Anil Aswani, Humberto Gonzalez, S Shankar Sastry, and Claire Tomlin. Provably safe and robust learning-based model predictive control. *Automatica*, 49(5):1216–1226, 2013.

Dan Barnes, Will Maddern, and Ingmar Posner. Find your own way: Weakly-supervised segmentation of path proposals for urban autonomy. In *2017 IEEE International Conference on Robotics and Automation (ICRA)*, pages 203–210. IEEE, 2017.

Felix Berkenkamp, Riccardo Moriconi, Angela P Schoellig, and Andreas Krause. Safe learning of regions of attraction for uncertain, nonlinear systems with gaussian processes. In *Conference on Decision and Control*, pages 4661–4666. IEEE, 2016.

Liyun Dai, Ting Gan, Bican Xia, and Naijun Zhan. Barrier certificates revisited. *Journal of Symbolic Computation*, 80:62–86, 2017.

Sarah Dean and Benjamin Recht. Certainty equivalent perception-based control. In *Learning for Dynamics and Control*, pages 399–411. PMLR, 2021.

Sarah Dean, Nikolai Matni, Benjamin Recht, and Vickie Ye. Robust guarantees for perception-based control. In *Learning for Dynamics and Control*, pages 350–360. PMLR, 2020.

Sarah Dean, Andrew Taylor, Ryan Cosner, Benjamin Recht, and Aaron Ames. Guaranteeing safety of learned perception modules via measurement-robust control barrier functions. In *Conference on Robot Learning*, pages 654–670. PMLR, 2021.

Yarin Gal and Zoubin Ghahramani. Dropout as a bayesian approximation: Representing model uncertainty in deep learning. In *international conference on machine learning*, pages 1050–1059. PMLR, 2016.

Lukas Hewing, Kim P Wabersich, Marcel Menner, and Melanie N Zeilinger. Learning-based model predictive control: Toward safe learning in control. *Annual Review of Control, Robotics, and Autonomous Systems*, 3:269–296, 2020.

Haimin Hu, Mahyar Fazlyab, Manfred Morari, and George J Pappas. Reach-sdp: Reachability analysis of closed-loop systems with neural network controllers via semidefinite programming. In *2020 59th IEEE Conference on Decision and Control (CDC)*, pages 5929–5934. IEEE, 2020.

Yihan Hu, Jiazhi Yang, Li Chen, Keyu Li, Chonghao Sima, Xizhou Zhu, Siqi Chai, Senyao Du, Tianwei Lin, Wenhai Wang, et al. Planning-oriented autonomous driving. In *Proceedings of the IEEE/CVF Conference on Computer Vision and Pattern Recognition*, pages 17853–17862, 2023.

Yann LeCun, Yoshua Bengio, and Geoffrey Hinton. Deep learning. *nature*, 521(7553):436–444, 2015.

Xiao Li, Yidong Du, Zhen Zeng, and Odest Chadwicke Jenkins. Seannet: Semantic understanding network for localization under object dynamics. *arXiv preprint arXiv:2110.02276*, 2021.

Xiao Li, Yutong Li, Nan Li, Anouck Girard, and Ilya Kolmanovsky. Set-theoretic localization for mobile robots with infrastructure-based sensing. *Advanced Control for Applications: Engineering and Industrial Systems*, 5(1):e117, 2023.

Johan Lofberg. Yalmip: A toolbox for modeling and optimization in matlab. In *2004 IEEE international conference on robotics and automation (IEEE Cat. No. 04CH37508)*, pages 284–289. IEEE, 2004.

Adam Paszke, Sam Gross, Francisco Massa, Adam Lerer, James Bradbury, Gregory Chanan, Trevor Killeen, Zeming Lin, Natalia Gimelshein, Luca Antiga, et al. Pytorch: An imperative style, high-performance deep learning library. *Advances in Neural Information Processing Systems*, 32, 2019.

Thomas Roddick and Roberto Cipolla. Predicting semantic map representations from images using pyramid occupancy networks. In *Proceedings of the IEEE/CVF Conference on Computer Vision and Pattern Recognition*, pages 11138–11147, 2020.

Alexander Shkolnik, Matthew Walter, and Russ Tedrake. Reachability-guided sampling for planning under differential constraints. In *2009 IEEE International Conference on Robotics and Automation*, pages 2859–2865. IEEE, 2009.

Vincent Tjeng, Kai Xiao, and Russ Tedrake. Evaluating robustness of neural networks with mixed integer programming. *arXiv preprint arXiv:1711.07356*, 2017.

Mukun Tong, Charles Dawson, and Chuchu Fan. Enforcing safety for vision-based controllers via control barrier functions and neural radiance fields. In *2023 IEEE International Conference on Robotics and Automation (ICRA)*, pages 10511–10517. IEEE, 2023.

Li Wang, Dongkun Han, and Magnus Egerstedt. Permissive barrier certificates for safe stabilization using sum-of-squares. In *2018 Annual American Control Conference (ACC)*, pages 585–590. IEEE, 2018.

Tianhao Wei and Changliu Liu. Safe control with neural network dynamic models. *arXiv preprint arXiv:2110.01110*, 2021.

Appendix A. Formal Safety Guarantee

The proofs of Proposition 1, 2, 3 are presented in A.1, A.2, A.3, respectively. Subsequently, the hypercube defined by the lower and upper bounds $\underline{x}_{k+1}, \overline{x}_{k+1}$, as a result of the MILP problem (17), contains the actual state x_{k+1}, and the hypercube is within the safe set $\mathcal{X}_s$, i.e., $x_{k+1} \in [\underline{x}_{k+1}, \overline{x}_{k+1}] \subset \mathcal{X}_s$. This proves Proposition 4.

A.1. Input Constraints

Proof Based on assumption in (3) and $x_k \in \mathcal{X}_s \subset \mathcal{X}$, it's obvious that $x_k \in \mathcal{X}_k = (y_k \ominus \mathcal{W}_y) \cap \mathcal{X}_s$ by the definition of Pontryagin difference, thereby we have $x_k \in \mathcal{X}_k \subset (y_k \ominus \mathcal{W}_y) \cap \mathcal{X}$. As defined in (9) together with the hypercube assumptions in (6b), (8a), the following statement can be proved

$$\forall x \in (y_k \ominus \mathcal{W}_y) \cap \mathcal{X},\ a_{0,1:n_x} = \max\{\underline{x}, y_k - \epsilon^y\} \leq x \leq \min\{\overline{x}, y_k + \epsilon^y\} = b_{0,1:n_x}.$$

Therefore, we can conclude that

$$x_k \in [a_{0,1:n_x},\ b_{0,1:n_x}]\,. \tag{18}$$

Similarly, based on (4) and $u_k \in \mathcal{U}$, we can show that $u_k \in \mathcal{U}_k$ and $\max\{\underline{u}, \tilde{u}_k - \epsilon^u\} \leq u \leq \min\{\overline{u}, \tilde{u}_k + \epsilon^u\}$ for all $u \in \mathcal{U}_k$. Next, we need to show that the constraints (10) imply $a_{0,(n_x+1):(n_x+n_u)} = \max\{\underline{u}, \tilde{u}_k - \epsilon^u\}$ and $b_{0,(n_x+1):(n_x+n_u)} = \min\{\overline{u}, \tilde{u}_k + \epsilon^u\}$ from which we can conclude

$$u_k \in \left[a_{0,(n_x+1):(n_x+n_u)},\ b_{0,(n_x+1):(n_x+n_u)}\right]. \tag{19}$$

If $\delta^a_j = 1$, the constraints (10) yield the following inequalities

$$\begin{cases} a_{0,j} \geq \underline{u}_j \\ a_{0,j} \geq \tilde{u}_{k,j} - \epsilon^u_j \\ a_{0,j} \leq \underline{u}_j \\ a_{0,j} \leq \tilde{u}_{k,j} - \epsilon^u_j + \max\{\epsilon^u_j, \overline{u}_j - \underline{u}_j - \epsilon^u_j\} \end{cases}$$

where the first three inequalities are equivalent to $a_{0,j} = \underline{u}_j,\ \underline{u}_j \geq \tilde{u}_{k,j} - \epsilon^u_j$. In this case, we have $a_{0,j} = \max\{\underline{u}_j, \tilde{u}_{k,j} - \epsilon^u_j\}$ and the fourth inequality is valid since $\underline{u}_j \leq \tilde{u}_{k,j} \leq \overline{u}_j$ and $a_{0,j} - \tilde{u}_{k,j} + \epsilon^u_j \leq \underline{u}_j - \underline{u}_j + \epsilon^u_j \leq \epsilon^u_j \leq \max\{\epsilon^u_j, \overline{u}_j - \underline{u}_j - \epsilon^u_j\}$.

If $\delta^a_j = 0$, the constraints (10) produce the following inequalities

$$\begin{cases} a_{0,j} \geq \underline{u}_j \\ a_{0,j} \geq \tilde{u}_{k,j} - \epsilon^u_j \\ a_{0,j} \leq \tilde{u}_{k,j} - \epsilon^u_j \\ a_{0,j} \leq \underline{u}_j + \max\{\epsilon^u_j, \overline{u}_j - \underline{u}_j - \epsilon^u_j\} \end{cases}$$

where the first three inequalities are equivalent to $a_{0,j} = \tilde{u}_{k,j} - \epsilon^u_j,\ \tilde{u}_{k,j} - \epsilon^u_j \geq \underline{u}_j$. Again, we can show $a_{0,j} = \max\{\underline{u}_j, \tilde{u}_{k,j} - \epsilon^u_j\}$ and the fourth inequality is also feasible since $a_{0,j} - \underline{u}_j = \tilde{u}_{k,j} - \epsilon^u_j - \underline{u}_j \leq \overline{u}_j - \epsilon^u_j - \underline{u}_j \leq \max\{\epsilon^u_j, \overline{u}_j - \underline{u}_j - \epsilon^u_j\}$.

Hence, we can conclude that $a_{0,j} = \max\{\underline{u}_j, \tilde{u}_{k,j} - \epsilon^u_j\}$ for $j = (n_x + 1), \ldots, (n_x + n_u)$ that is equivalent to $a_{0,(n_x+1):(n_x+n_u)} = \max\{\underline{u}, \tilde{u}_k - \epsilon^u\}$ and the proof of $b_{0,(n_x+1):(n_x+n_u)} = \min\{\overline{u}, \tilde{u}_k + \epsilon^u\}$ resembles the discussion above. Eventually, based on (18) and (19), the input z_0 to the NN satisfies

$$z_0 = [x_k^T\ u_k^T]^T \in [a_0,\ b_0]\,. \tag{20}$$

■

A.2. NN Structural Constraints

Proof We first provide proof of the following statement

$$\hat{z}_i = W^{(i)} z_{i-1} + b^{(i)} \in \left[\hat{a}_i,\ \hat{b}_i\right],\ z_i = \max\{0,\ \hat{z}_i\} \in [a_i,\ b_i],\ \text{given } z_{i-1} \in [a_{i-1},\ b_{i-1}].$$

Then, from the results $z_0 \in [a_0,\ b_0]$ in (20), we can inductively prove the same argument for $i = 1, \ldots, \ell - 1$.

Given $z_{i-1} \in [a_{i-1},\ b_{i-1}]$, the j^{th} element in $\hat{z}_i$ is $\hat{z}_{i,j} = w_j^{(i)} z_{i-1} + b_j^{(i)}$ where $w_j^{(i)} = [w_1 \ldots w_q \ldots w_{n_{i-1}}]$ and satisfies the following inequalities

$$\begin{aligned}
&\sum_{q=1}^{n_{i-1}} \left([\![w_q \geq 0]\!] \cdot (w_q a_{i-1,q}) + [\![w_q < 0]\!] \cdot (w_q b_{i-1,q})\right) \\
&\qquad \leq \hat{z}_{i,j} - b_j^{(i)} \leq \\
&\sum_{q=1}^{n_{i-1}} \left([\![w_q \geq 0]\!] \cdot (w_q b_{i-1,q}) + [\![w_q < 0]\!] \cdot (w_q a_{i-1,q})\right),
\end{aligned}$$

where the Iverson bracket $[\![\cdot]\!]$ takes the value of 1 if the statement inside is true and 0 otherwise. We can derive the following equalities from the constraints in (11)

$$\begin{aligned}
\hat{a}_{i,j} - b_j^{(i)} &= \sum_{q=1}^{n_{i-1}} \left([\![w_q \geq 0]\!] \cdot (w_q a_{i-1,q}) + [\![w_q < 0]\!] \cdot (w_q b_{i-1,q})\right), \\
\hat{b}_{i,j} - b_j^{(i)} &= \sum_{q=1}^{n_{i-1}} \left([\![w_q \geq 0]\!] \cdot (w_q b_{i-1,q}) + [\![w_q < 0]\!] \cdot (w_q a_{i-1,q})\right),
\end{aligned}$$

which implies

$$\hat{z}_{i,j} \in \left[\hat{a}_{i,j},\ \hat{b}_{i,j}\right],\ j = 1, \ldots, n_i. \tag{21}$$

Afterward, given $\underline{\hat{z}}_{i,j} \leq \hat{a}_{i,j} \leq \hat{z}_{i,j} \leq \hat{b}_{i,j} \leq \overline{\hat{z}}_{i,j}$ in (11) and constraints in (12), we need to prove $a_{i,j} \leq z_{i,j} \leq b_{i,j}$. If $\delta_{i,j}^{--} = 1$, the constraints in (12) are reduced to

$$\begin{cases}
b_{i,j} \geq a_{i,j} \geq 0 \\
\hat{a}_{i,j} \leq a_{i,j} \leq 0 \\
\hat{b}_{i,j} \leq b_{i,j} \leq 0 \\
a_{i,j} \leq \hat{a}_{i,j} - \underline{\hat{z}}_{i,j} \\
b_{i,j} \leq \hat{b}_{i,j} - \underline{\hat{z}}_{i,j}
\end{cases}.$$

The first three inequalities are equivalent to $a_{i,j} = b_{i,j} = 0$, $\hat{a}_{i,j} \leq 0$, $\hat{b}_{i,j} \leq 0$ which induce $\hat{z}_{i,j} \leq \hat{b}_{i,j} \leq 0$ and $z_{i,j} = \max\{0,\ \hat{z}_{i,j}\} = 0$, thereby we have $0 = a_{i,j} \leq z_{i,j} \leq b_{i,j} = 0$. Meanwhile, the last two inequalities hold since $\underline{\hat{z}}_{i,j} \leq \hat{a}_{i,j} \leq \hat{z}_{i,j} \leq \hat{b}_{i,j} \leq \overline{\hat{z}}_{i,j}$.

If $\delta_{i,j}^{-+} = 1$, the constraints in (12) are reduced to

$$\begin{cases}
b_{i,j} \geq a_{i,j} \geq 0 \\
\hat{a}_{i,j} \leq a_{i,j} \leq 0 \\
\hat{b}_{i,j} \leq b_{i,j} \leq \hat{b}_{i,j} \\
a_{i,j} \leq \hat{a}_{i,j} - \underline{\hat{z}}_{i,j} \\
b_{i,j} \leq \overline{\hat{z}}_{i,j}
\end{cases}.$$

The first three inequalities imply that $a_{i,j} = 0$, $\hat{a}_{i,j} \leq 0$ and $b_{i,j} = \hat{b}_{i,j}$, $\hat{b}_{i,j} \geq 0$ from which we can show that $0 \leq z_{i,j} \leq \hat{b}_{i,j}$. Thus, we have $a_{i,j} = 0 \leq z_{i,j} \leq \hat{b}_{i,j} = b_{i,j}$ and the last two inequalities are also feasible.

If $\delta_{i,j}^{++} = 1$, the constraints in (12) are reduced to

$$\begin{cases} b_{i,j} \geq a_{i,j} \geq 0 \\ \hat{a}_{i,j} \leq a_{i,j} \leq \hat{a}_{i,j} \\ \hat{b}_{i,j} \leq b_{i,j} \leq \hat{b}_{i,j} \\ a_{i,j} \leq \overline{\hat{z}}_{i,j} \\ b_{i,j} \leq \overline{\hat{z}}_{i,j} \end{cases}.$$

The first three inequalities imply that $a_{i,j} = \hat{a}_{i,j}$, $\hat{a}_{i,j} \geq 0$ and $b_{i,j} = \hat{b}_{i,j}$, $\hat{b}_{i,j} \geq 0$ from which we can show $\hat{a}_{i,j} \leq z_{i,j} \leq \hat{b}_{i,j}$. Thus, we have $a_{i,j} = \hat{a}_{i,j} \leq z_{i,j} \leq \hat{b}_{i,j} = b_{i,j}$ and the last two inequalities are valid. To this end, we have proven that

$$z_{i,j} \in [a_{i,j},\ b_{i,j}]\,,\ j = 1, \ldots, n_i. \tag{22}$$

Indeed, as discussed at the beginning of this section, we can show that

$$\hat{z}_i \in \left[\hat{a}_i,\ \hat{b}_i\right],\ z_i \in [a_i,\ b_i]\,,\ i = 1, \ldots, \ell - 1 \tag{23}$$

with (20). Identical to the proof of (21), given $z_{\ell-1} \in [a_{\ell-1},\ b_{\ell-1}]$ in (23), constraints in (13) and $\tilde{x}_{k+1} = W^{(\ell)} z_{\ell-1} + b^{(\ell)}$ in (1), we can demonstrate that

$$\tilde{x}_{k+1} \in \tilde{\mathcal{F}}(\mathcal{X}_k, \mathcal{U}_k) \subseteq [a_{k+1},\ b_{k+1}]\,. \tag{24}$$

■

A.3. Output Constraints

Proof With the assumptions in (2) and (6a), we can show $x_{k+1} \in [a_{k+1},\ b_{k+1}] \oplus \mathcal{W}_x$ which can be further derived to

$$x_{k+1} \in \left[\underline{x}_{k+1},\ \overline{x}_{k+1}\right] \subset \mathcal{X}, \tag{25}$$

based on the constraints in (14). Meanwhile, the constraints in (15) are equivalent to the following statement

$$\exists j \in \{1, \ldots, n_x\},\ s.t.\ \delta_{1,j}^u = 1 \text{ or } \delta_{2,j}^u = 1.$$

In the sequel, we show that $\left[\underline{x}_{k+1},\ \overline{x}_{k+1}\right] \cap \mathcal{X}_u = \varnothing$ with constraints in (15) if $\delta_{1,j}^u = 1$ which the proof resembles in case of $\delta_{2,j}^u = 1$. If $\delta_{1,j}^u = 1$, the constraints in (15) can be reformulated into

$$\underline{x}_j \leq \underline{x}_{k+1,j} \leq \overline{x}_{k+1,j} \leq \underline{x}_{u,j}.$$

Suppose $\left[\underline{x}_{k+1},\ \overline{x}_{k+1}\right] \cap \mathcal{X}_u \neq \varnothing$, therefore there exists $x^* = [x_1^* \cdots x_j^* \cdots x_{n_x}^*]^T \in \mathbb{R}^{n_x}$ such that $x^* \in \left[\underline{x}_{k+1},\ \overline{x}_{k+1}\right] \cap \mathcal{X}_u$. Then, for some index j and $1 \leq j \leq n_x$, we have $\underline{x}_{u,j} \leq x_j^* \leq \overline{x}_{u,j}$ and $\underline{x}_{k+1,j} \leq x_j^* \leq \overline{x}_{k+1,j}$ which violates $\overline{x}_{k+1,j} \leq \underline{x}_{u,j}$. By contradiction, the following is true

$$\left[\underline{x}_{k+1},\ \overline{x}_{k+1}\right] \cap \mathcal{X}_u = \varnothing. \tag{26}$$

With equations (25) and (26), we demonstrate that $x_{k+1} \in \mathcal{F}(\mathcal{X}_k, \mathcal{U}_k) \subseteq [\underline{x}_{k+1}, \overline{x}_{k+1}] \subset \mathcal{X}_s$ which complete the proof for Proposition 3. ■